The effect of oxygen in the photocatalytic oxidation pathways of perfluorooctanoic acid

Maurizio Sansotera[a,b], Federico Persico[a], Valentina Rizzi[a], Walter Panzeri[c], Carlo Pirola[b,d], Claudia L. Bianchi[b,d], Andrea Mele[a,b], Walter Navarrini[a,b,*]

[a] *Dipartimento di Chimica, Materiali e Ingegneria Chimica "Giulio Natta", Politecnico di Milano, Via Mancinelli 7, 20131, Milano, Italy*

[b] *Consorzio Interuniversitario Nazionale per la Scienza e Tecnologia dei Materiali (INSTM), Via G. Giusti 9, 50121, Firenze, Italy*

[c] *C.N.R. - Consiglio Nazionale delle Ricerche, Istituto di Chimica del Riconoscimento Molecolare, Sezione "U.O.S. Milano Politecnico", Via Mancinelli 7, 20131, Milano, Italy*

[d] *Dipartimento di Chimica, Università degli Studi di Milano, Via Golgi 19, 20133, Milano, Italy*

* Corresponding author. Tel: +39.02.2399.3029; Fax: +39.02.2399.3180; Email Address: walter.navarrini@polimi.it

Abstract

The influence of oxygen in the photocatalytic oxidation of perfluorooctanoic acid (PFOA) promoted by a commercial nano-sized titanium dioxide was studied by testing the reaction in different conditions: static air, oxygen flux, nitrogen flux and pre-saturated nitrogen flux. The reaction was monitored by Total Organic Carbon (TOC) analysis and Ionic Chromatography (IC). Shorter chain perfluorocarboxylic acids (PFCAs; C_n, n = 1-7) intermediate degradation products were quantitatively determined by High-Performance Liquid Chromatography combined with Mass Spectrometry (HPLC-MS) analysis. The presence of shorter chain PFCAs in solution was also monitored by ^{19}F-NMR. The experimental findings are in agreement with two major oxidative

pathways: $C_n \rightarrow C_{n-1}$ photo-redox and β-scissions routes mediated by COF_2 elimination. Depending on the experimental conditions, the mutually operating mechanisms could be unbalanced up to the complete predominance of one pathway over the other. In particular, the existence of the β-scissions route with COF_2 elimination was corroborated by the isolation and characterization of carbonyl difluoride, a predicted fluorinated decomposition by-product.

Keywords: PFOA, Oxidation, Titanium dioxide, Photocatalysis, Carbonyl difluoride

1. Introduction

PFOA and its salts are exogenous very stable perfluorinated surfactants, utilized till now for the preparation of the majority of fluoropolymers that are worldwide employed in thousands of everyday life essential applications, such as manufacturing, aerospace, automotive, electronics, semiconductors and textile [1]. PFOA UV stability and high surface-active effects are due to its completely perfluorinated structure [2-4]. However, perfluorocarboxylic acids (PFCAs) are nowadays source of great concern due to their proved persistence in the global abiotic and biotic environment, including food and humans [5-7]. These compounds, in fact, are among the most widely diffused fluorinated surfactants into waste streams [8-10].

The 2015 is the deadline for the complete phase out of perfluorooctanoic acid; this phase out plane was launched in the PFOA Stewardship Program by US-EPA and by eight major companies in 2006 [1]. As a direct consequence of this program, the fluoropolymer industry has been forced to develop new environmentally friendly surfactants suitable for emulsion polymerization. In addition, from that moment on, many important research studies on PFOA substitutes and related materials appeared in the specialized literature [11-17]. Furthermore, due to recent findings on the extreme difficulty to decompose PFOA by using standard methodologies, new and effective degradation techniques like electrochemical [18], modified Fenton reagent [19], sonochemical [20], plasma [21], microwave [22], photochemical [23,24] and photocatalytic methods [25-29] have been studied

and published. In addition extensive technological reviews are also available in the literature [30-32].

In this study, we analyzed the influence of oxygen in PFOA photocatalytic oxidation induced by UV-activated TiO_2. Semiconductors, in particular TiO_2, are characterized by an electronic band structure in which electrons from the valence band (V_b) are promoted to the conductive band (C_b) with the simultaneous generation of positively charged holes (h^+) in the V_b by the absorption of a photon flux of energy equal or higher to the bandgap energy. The electron-hole pairs can recombine in a few nanoseconds, or they can be trapped in surface states where they can react with donor or acceptor species adsorbed on the photocatalyst surface [33]. Interface redox reactions involving both excited electrons and photogenerated holes must compete effectively with the recombination processes of the electron-hole pairs [34,35]. In the presence of water and oxygen, hydroxyl radicals ·OH and superoxide ions $O_2^{-}\cdot$ are generated [36]. These intermediates are strong oxidizing species able to mineralize organic compounds [37,38]. However, an extensive debate on the oxidative pathway of PFOA exists nowadays, because it has been demonstrated that ·OH radicals generated by Fenton reagent are not very effective in the PFOA mineralization [30,39] and that $Ti^{IV}OH^{\cdot+}$ can take an active part in the mineralization reaction [27,40,41].

Despite the numerous studies on PFOA oxidation, at the moment a complete rationalization of the decomposition pathways is not available. The interpretation of experimental findings, as well as *a priori* calculations reported in the literature, are often in apparent contradiction [19,26,30] and provide an incomplete interpretation of the PFOA oxidation mechanism [25] or, in some cases, the experimental findings are complementary [18,21]. The intent of this work is to give our contribution to the understanding of this intriguing reaction. In particular, we focused on the influence of oxygen in the photocatalytic oxidation of PFOA induced by UV-activated TiO_2 and we obtained that, differently from static conditions, a continuous oxygen feeding enhanced the decomposition of PFOA till its mineralization. On the contrary, PFOA photooxidation was hindered in a nitrogen-saturated reaction environment.

The use of oxygen excess directed the PFOA decomposition through a reaction pathway involving the formation of oxygen-centered perfluorinated radicals as major intermediates. As already hypothesized, the perfluorinated oxyradicals preferentially followed a β-scission route by releasing carbonyl difluoride, COF_2, as a specific by-product, which can be hardly isolated due to its rapid hydrolysis in aqueous media [42]. Carbonyl difluoride is an important intermediate for the industrial synthesis of key fluorinated monomers and it is essential in the preparation of fluoroplastics and perfluororubbers [43-45]. In this work, we firstly report that the intermediate COF_2 can be isolated in pure form and in good selectivity by performing the photocatalytic oxidation of PFOA in a suitable perfluorinated aprotic solvent, instead of water. Moreover, in these conditions the catalyst deactivation due to fluoride ions is mostly inhibited [27]. As often happens, a more complete understanding of a reaction mechanism gives more options in the utility of the reaction under study [46,47]. In particular, in the photocatalytic oxidation of PFOA a new chemical route has been identified for the synthesis of carbonyl difluoride, COF_2.

2. Materials and methods

2.1. Materials

Perfluorooctanoic acid (purity 96% - from Sigma Aldrich®) was used as received. PFOA is soluble in water (9.5 g/L) and its critical micelle concentration (CMC) is $7.80 \cdot 10^{-3}$ mol/L at 25°C [48]. Titanium dioxide P-25 (75% Anatase, 25% Rutile) was supplied by Evonik® and it was tested as a titanium-based photocatalyst. The coexistence of anatase and rutile in commercial P-25 causes the catalyst photoactivity to be enhanced if compared to pure anatase [49]. The presence of small rutile crystallites, in fact, creates a structure characterized by a more stable charge separation, slowing recombination reactions on anatase; moreover, the smaller band gap of rutile extends the useful range of photoactivity into the visible region [49]. Water was purified by using an Elga Option 3 deionizer and it was used to prepare PFOA solutions for the different kinetic tests. Milli-Q water was employed for ion chromatography. HPLC-MS analyses were carried out by using as an eluting

phase a mixture of methanol (CHROMASOLV®, for HPLC, ≥ 99.9% - from Sigma Aldrich®) and 2 mM aqueous ammonium acetate solution. The evaluation of COF_2 formation during PFOA abatement was specifically monitored by degrading a solution of PFOA in Galden® HT-170 (from Solvay Specialty Polymers), a PFPE-based solvent with boiling point of 170°C and formula as follows: $CF_3O(CF_2CF(CF_3)O)_p(CF_2O)_nCF_3$ (AMW = 760).

2.2. Photocatalysis

The photocatalytic apparatus was a 1 L glass stirred reactor equipped with an iron halogenide UV lamp (500 W, Jelosil® HG500) emitting light at wavelengths of 315-400 nm and able to irradiate the reactor with a specific power of 75 W/m^2. The UV lamp was placed beside the reactor, which was cooled with water at a temperature of 30.0 ± 0.5°C [27]. Titanium dioxide was introduced in the reactor at the beginning of each test (0.66 g/L) [27]. The variation of the surfactant concentration in solution was monitored by Total Organic Carbon (TOC) analysis and Ionic Chromatography [27]. The PFOA initial concentration ($[PFOA]_0$ = 4 mM) was maintained lower than its CMC (7.8 mM [48]) in order to avoid the formation of emulsions that would reduce the TiO_2-promoted photodegradation rates [27,28]. Moreover, the PFOA initial concentration was high enough to allow the detection of the degradation intermediates, even at very low concentrations. Each kinetic test was repeated three times in order to evaluate the error extent and realized by collecting samples (10 ml) of the reaction mixture at predetermined reaction times. Samples were centrifuged and filtered through a 0.45 μm polycarbonate membrane in order to separate the TiO_2 powder from the solution. Photocatalytic process could be commonly described in terms of a modified Langmuir-Hinshelwood (L-H) model, which has been successfully used for heterogeneous photocatalytic degradation by determining the relationship between the apparent first-order rate constant and the initial content of the organic substrate [50,51]:

$$r = -\frac{dC}{dt} = \frac{k_r K_S C}{1 + K_S C_0} = k_{app} C \qquad (1)$$

In Equation 1, r is the reaction rate, C is the pollutant concentration in solution, C_0 is the initial organic content, k_r is the reaction rate constant, K_S is the adsorption rate constant, t is the time and k_{app} the apparent first-order rate constant. In the original L-H model the rate constant k_r and the adsorption constant K_S are independent of light intensity and K_S should not vary with the light intensity because it represents the adsorptive affinity of a substrate on the catalyst surface. Differently, in the modified L-H model the light intensity can affect both kinetic constants (k_r, K_S), as reported in the literature [50,51].

The effects on PFOA photocatalytic oxidation due to both oxygen excess and deficiency in the reaction environment were evaluated by running and comparing the results of specific kinetic tests; in particular, PFOA degradation trends were monitored in atmospheric conditions (*Air test*), in the presence of a constant O_2 flux (*O_2 test* - F_{O2} = 7 NL/h) and in the presence of a constant N_2 flux (F_{N2} = 7 NL/h). The latter case comprehended two different oxygen starvation tests: PFOA degradation under N_2 flux with an air-saturated initial solution (*N_2 test*) and with a N_2-presaturated reaction environment (*N_{2sat} test* - PFOA solution fluxed with N_2 for 12 h until saturation, then F_{N2} = 7 NL/h during the kinetic test). Dark and photolysis tests were also conducted (Table S.I.9 and Table S.I.10, respectively).

In order to verify the deactivating effect of fluoride ions towards TiO_2, an additional test (*F^- test*) was performed by adding potassium fluoride ($[KF]_0$ = 120 mM) to the initial PFOA solution. In these conditions PFOA photoabatement was not observed, thus confirming the effects due to the fluoride-promoted deactivation of the catalyst (see Table S.I.11 in the Supporting Information for more details).

2.3. Detection of carbonyl difluoride

The intent of this test was the detection of COF_2, hypothesized as a specific by-product in the PFOA degradation pathway based on the β-scission reaction. The photocatalytic apparatus described in Paragraph 3.2 was connected to an on-line Thermo Nicolet 380 FT-IR set with a PTFE

gas-tight IR cell (volume 8 cm^3, length 10 cm) equipped with CaF_2 windows. The outlet gases of the cell were neutralized in a saturated $NaHCO_3$ aqueous solution. PFOA ($[PFOA]_0$ = 4 mM) was dissolved in a high boiling point PFPE-based solvent (Galden® HT-170) and this solution was introduced in the reactor. The use of aqueous solutions in the photoabatement of PFOA did not allow the detection of COF_2 because of its rapid hydrolysis. Titanium dioxide P-25 (0.66 g/L) was used as a photocatalyst and the UV lamp (75 W/m^2) was placed beside the reactor. Oxygen (F_{O2} = 7 NL/h) was continuously fluxed in the reactor. FT-IR analysis was used to monitor the composition of the outlet gases and to verify the formation of COF_2, by comparing its typical IR signal at 1928 cm^{-1} due to the C=O stretching (Table S.I.12). The concentration of COF_2 (expressed in parts per million by volume, ppmV) was calculated on the basis of its reported molar absorptivity at 10110 cm/mmol [42]. A portion of the outlet gases was bubbled in a NMR tube containing toluene-d_8 cooled in a dry ice-acetone bath at -78°C [52]. ^{19}F-NMR spectrum was recorded on a Bruker 500 Ultrashield spectrometer operating at 470.30 MHz and 305 K.

Chemical stability test of pure Galden® HT-170 towards UV-activated TiO_2 and dark test of a PFOA solution in Galden® HT-170 were also performed under O_2 flux (F_{O2} = 7 NL/h - see Tables S.I.13 and S.I.14 in the Supporting Information for more details).

2.4. TOC analysis and ion chromatography

Total Organic Carbon (TOC) analysis allowed to evaluate and to monitor the trend of the carbon content of the solution. TOC analyses were performed with a Shimadzu® TOC 5000 A with a combustion/non-dispersive infrared (NDIR) gas analysis method. The total organic carbon concentration of the PFOA solution at different photodegradation times was calculated automatically by comparing the sample with a calibration curve obtained from PFOA solutions at defined concentrations. In the kinetic study of PFOA degradation, the data obtained by TOC analysis were considered for the calculation of C/C_0 ratios. The PFOA degradation generated

fluoride ions in solution and their concentration was monitored by Ion Chromatography (IC) with a Metrohm 883 Basic IC Plus.

2.5. High-Performance Liquid Chromatography with Mass Spectrometry (HPLC-MS)

Analytes separation was performed by using an Agilent 1100 Series HPLC Value System, consisting of a quaternary pump, vacuum degasser and auto sampler. The instrument was equipped with a Lichrocart® 55-4 Purospher® STAR RP-18 end capped column (55 x 4.0 mm i.d., 3 μm) supplied by Merck KGaA. For quantitative determination, the chromatographic system was interfaced to a Bruker Esquire 3000 Plus quadrupole ion trap mass spectrometer (Bruker Daltonics) operating in negative electrospray mode. Instrumental parameters were optimized to transmit the $[M-H]^-$ ions for all expected degradation intermediates. Primary ions monitored for PFOA, perfluoroheptanoic acid (PFHpA), perfluorohexanoic acid (PFHxA), perfluoropentanoic acid (PFPeA), perfluorobutanoic acid (PFBA), perfluoropropionic acid (PFPrA) and trifluoroacetic acid (TFA) determinations were 413, 363, 313, 263, 213, 163 and 113 $[M-H]^-$, respectively (see Appendix A). Samples of the reaction mixture collected at different reaction times were diluted in deionized water (1:10) and injected in the HPLC-MS with 2 mM ammonium acetate/methanol as the mobile phase starting at 10% methanol, at a flow rate of 200 μL/min. The gradient increased to 90% methanol at 5 min; before reverting to original conditions at 20 min, the gradient decreased to 80% methanol at 15 min. Column temperature was maintained at 40°C. HPLC-MS spectrum of *Air Test* sample collected after 7 h and the extractions of primary ions due to PFOA and degradation PFCA intermediates are reported as example in the Supporting Information (Fig. S.I.1).

2.6. Fluorine-19 nuclear magnetic resonance (^{19}F-NMR) spectroscopy

^{19}F-NMR tests were performed on a Bruker 500 Ultrashield spectrometer operating at 470.30 MHz and 305 K, in order to evaluate the trend of PFOA signals. In particular, for each kinetic test, the samples of solution collected from the photoabatement reactor at the beginning and at different

specific times were analyzed by ^{19}F-NMR, using D_2O as solvent. PFOA integral calculation allowed the detection of degradation products by considering the ratio between the integrals of the peaks ascribable to CF_3 groups, present in all the degradation by-products (C_2-C_7 perfluorinated acids; see Appendix A) and the integrals of the peaks ascribable to CF_2 signals.

2.7. X-ray photoelectron spectroscopy (XPS)

X-ray photoelectron spectroscopy spectra were obtained by using an M-probe apparatus (Surface Science Instruments). The source was monochromatic Al Kα radiation (1486.6 eV). A spot size of 200 μm x 750 μm and pass energy of 30 eV were used. *1s* level hydrocarbon-contaminant carbon was taken as the internal reference at 284.6 eV. Fittings were performed by using pure Gaussian peaks, Shirley's baseline, and without any constraints. X-ray photoelectron spectroscopy analysis was performed to study the composition of the photocatalyst surface after the photodegradation of a PFOA solution in Galden® HT-170. The TiO_2 sample for XPS analysis was obtained by centrifuging and filtering through a 0.45 μm polycarbonate membrane the surfactant solution at the end of the reaction (15 h); the sample was then dried in inert atmosphere for 24 hours and analyzed. High resolution XPS analyses in the typical zone of C *1s* (as reference) and Ti *2p* were performed.

3. Results and discussion

3.1. Photocatalytic oxidation of perfluorooctanoic acid

The solubility of perfluorocarboxylic acids can be approximated to their critical micelle concentration (CMC). In particular, PFOA is characterized by a CMC of 0.0078 M and above this value PFOA molecules tend to aggregate in micelles of average dimension around 100 nm, originating a colloid [48]. Below the CMC, PFOA molecules are expected to exhibit lower chemical stability than PFOA aggregates towards the coupled effect of TiO_2 and UV light [28]. On the basis of the optimizations achieved in previous studies [27,28], the general experimental conditions were maintained by setting PFOA initial concentration at 0.0040 M ($[PFOA]_0$ < CMC), TiO_2 content at

0.66 g/L and UV-lamp power at 75 W/m^2. Different kinetic tests were realized in order to evaluate the effects of oxygen excess or defect in the reaction environment. PFOA degradation trends were monitored in static conditions with atmospheric concentration of O_2 (*Air test*) and in the presence of a constant O_2 flux (*O_2 test* - F_{O2} = 7 NL/h) in order to obtain an O_2-enriched environment. Two kinetic tests were also run under N_2 flux in O_2 starvation conditions, either in the presence of residual oxygen traces due to the air-saturated initial solution (*N_2 test*) or in the complete absence of O_2 obtained by pre-saturating the PFOA solution with N_2 before starting the photocatalytic experiment (*N_{2sat} test* - see Paragraph 2.2 for details). The surfactant abatement trends were evaluated by monitoring at different times the mineralization percentage of the treated solutions by TOC analysis, the fluoride contents by IC analysis (Tables S.I.1, S.I.3, S.I.5 and S.I.7) and the degradation intermediates concentrations by HPLC-MS (Tables S.I.2, S.I.4, S.I.6 and S.I.8). PFOA concentrations expressed as ppm of carbon ascribed to PFOA and measured by HPLC-MS were reported for benchmarking purposes with the experimental TOC concentrations (Fig. 1-A). PFOA degradation kinetic data were interpolated by pseudo-first order curves ($R^2 > 0.96$) which enabled the comparison of the apparent rate constants, k_{app} (Fig. 1-B).

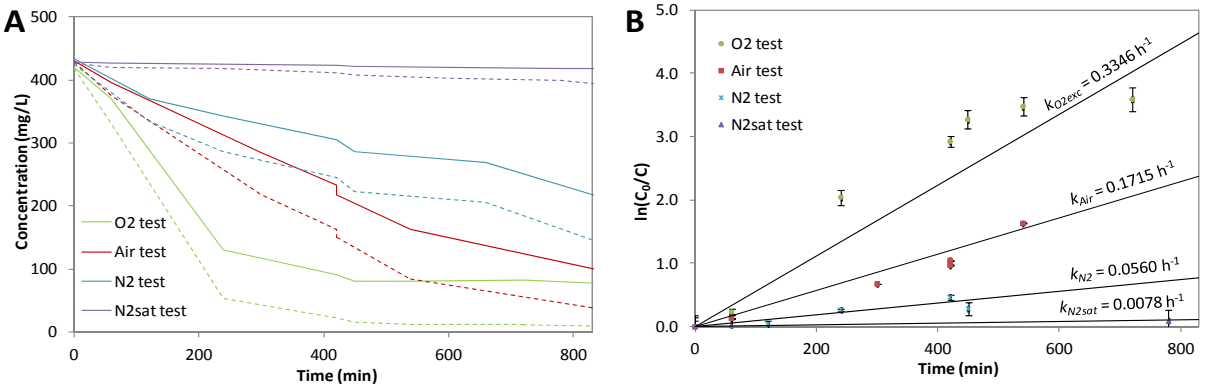

Figure 1. Concentration trends of TOC data (solid lines) compared to the ppm of carbon corresponding to PFOA concentration monitored by HPLC-MS (dashed lines) for the different kinetic tests (*O_2*, *Air*, *N_2* and *N_{2sat} test*) (A); linearization of PFOA degradation data obtained in the different kinetic tests (*O_2*, *Air*, *N_2* and *N_{2sat} test*) (B).

In the *Air test*, TOC content and PFOA concentration resulted to be constantly decreasing along the whole experiment and a substantially constant gap can be observed (Fig. 1-A). Considering the O_2 *test*, the total mineralization was very rapid during the first 4 h of abatement and after 7 h PFOA appeared to be almost completely degraded: $[PFOA]_{7h}/[PFOA]_0$ = 0.034. After 4 h, the mineralization rate clearly decreased, probably due to the F^--promoted chemical modifications of the catalyst surface [27]. The gap between the trends of TOC content and PFOA degradation was substantially constant after 7 h. The N_{2sat} *test* was run in N_2 pre-saturated reaction environment and a very low decrease in the TOC content was observed (Fig. 1-A): at the end of the test mineralization was slightly higher than 2%. Differently, the residual oxygen content present in the N_2 *test* due to the air-saturated initial solution raised the final mineralization to more than 50% and the PFOA abatement was about 71% (Fig. 1-A). These results are in complete agreement with the expected behavior of the system by supporting the enhancing role of oxygen in the reaction mechanism of PFOA photodegradation.

The linearization of PFOA degradation data are reported in Figure 1-B for all the experimental conditions tested, along with the calculated apparent kinetic constant. The apparent kinetic constant obtained in the O_2 *test* (k_{O2} = 0.3346 h^{-1}) was almost twice the one calculated in the *Air test* (k_{Air} = 0.1715 h^{-1}) (Fig.1-B). As expected, tests run in the presence of O_2 starvation (N_2 *test* and N_{2sat} *test*) allowed lower rates of PFOA removal (k_{N2} = 0.0560 h^{-1}, k_{N2sat} = 0.0078 h^{-1}). From the comparison of the calculated k_{app}, the importance of working in O_2-enriched conditions during PFOA photodegradation was confirmed. Moreover, no PFOA abatement was observed by working in the presence of TiO_2 as photocatalyst (0.66 g/L) without UV irradiation (*dark test,* Table S.I.9) or by working just under UV irradiation (75 W/m^2) without photocatalyst (*photolysis test,* Table S.I.10), in accordance to the literature [24]. The absence of any PFOA abatement in the dark test confirmed also that PFOA adsorption on the TiO_2 surface was negligible.

PFOA degradation intermediates were identified and quantified by HPLC-MS analysis. In the *Air test*, the concentration trends of the degradation intermediates in solution followed a well-defined

order: the higher the molecular weight of the intermediate, the higher its presence in solution (PFHpA > PFHxA > PFPeA > PFBA > PFPrA > TFA) (Fig. 2-A and 2-B). PFHpA concentration increased up to a maximum value (0.632 mM) followed by an evident decrease. This concentration trend can be related to the $C_n \rightarrow C_{n-1}$ chain length degradation pathway. It is important to notice that the shorter-chain acids formation during PFOA decomposition observed at the beginning of the reaction and the presence of TFA and PFPrA after 30 minutes (Fig. 2-B) cannot be ascribed to the generally accepted photo-redox consecutive $C_n \rightarrow C_{n-1}$ chain length decrease mechanism [29]. These findings can be justified by an alternative decomposition mechanism based on the elimination of COF_2 as a decomposition product induced by β-scission reactions of oxyradicals, in competition with the stepwise chain length decrease [28]. Overall, the concentration trends of PFOA degradation intermediates represented an indirect proof of the coexistence of two degradation pathways. In the *O_2 test*, PFHpA maximum concentration was comparable with the one observed in the *Air test*, as well as the final concentrations of PFHxA and PFPeA (Fig. 2-C and 2-D). On the contrary, PFPrA and TFA were definitely more concentrated at the end of the *O_2 test* than in the *Air test*. In the presence of O_2 excess, PFOA decrease appeared to be definitely more rapid and higher concentrations of short chain acids were detected. These results suggested that a PFOA oxidation mechanism alternative to the $C_n \rightarrow C_{n-1}$ stepwise chain length degradation should be considered, especially in the presence of appreciable O_2 concentrations. In the *N_2 test* (Fig. 2-E and 2-F), the formation of shorter-chain acids resulted greatly limited: $[PFPrA]_{max}$ and $[TFA]_{max}$ were 0.008 and 0.002 mM, respectively. In fact, in O_2 starvation, the PFOA abatement appeared to follow the generally accepted stepwise $C_n \rightarrow C_{n-1}$ chain length decrease mechanism and the PFOA concentration decreased constantly with gradual increase in C_7-C_6 acids content and relatively low formation of shorter chain acids. In *N_{2sat} test*, the very limited PFOA abatement (Fig. 1) and the related small increase in the PFOA degradation intermediates concentrations (Fig. 2-G and 2-H) were probably due to traces of oxidant species in the solution ascribable to residual O_2 or to the reaction between photogenerated holes and water adsorbed onto TiO_2 particles [53]. These

evidences overall suggest that the use of an external source of oxygen can promote the PFOA degradation.

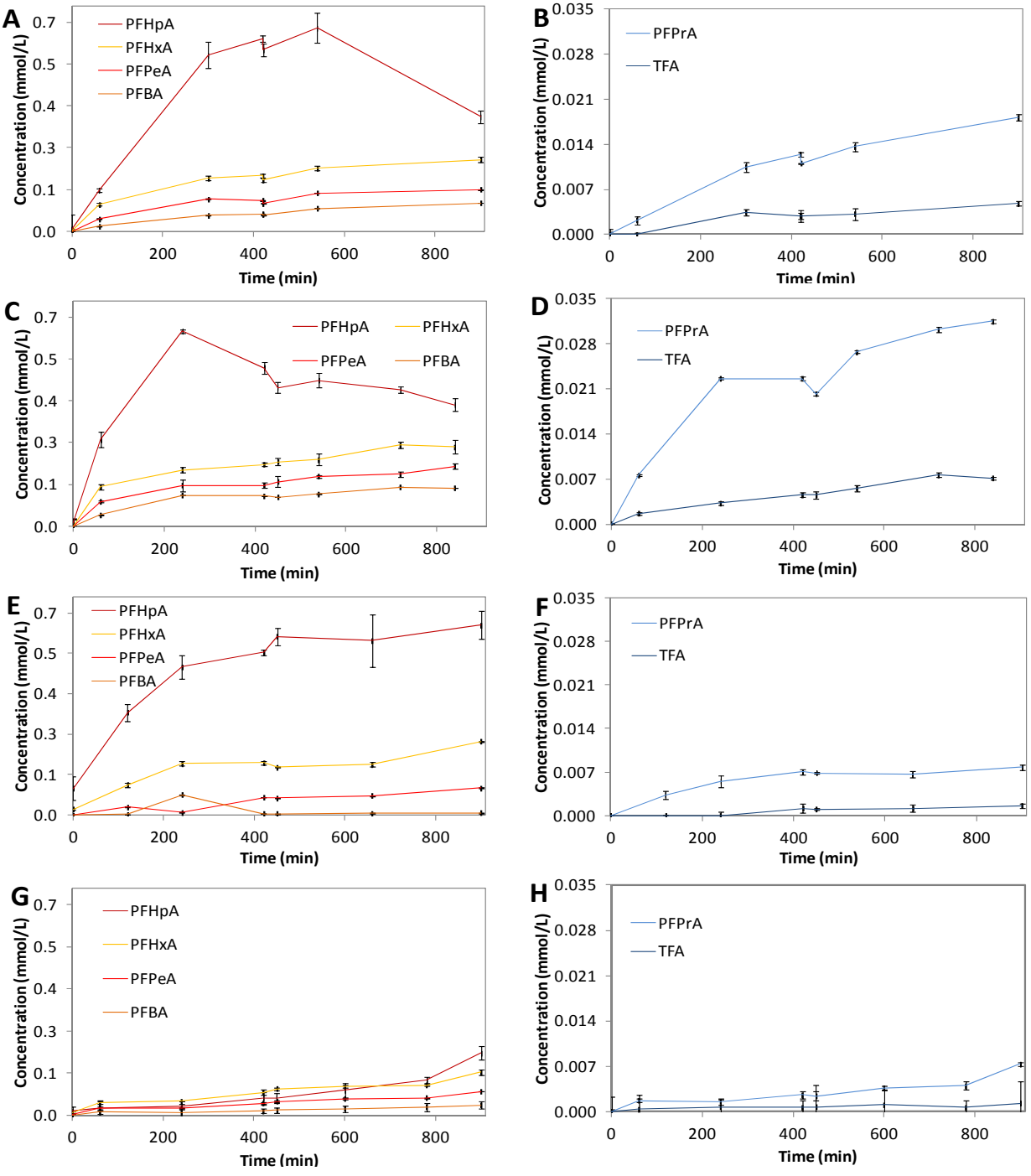

Figure 2. Concentration trends of PFOA degradation intermediates (PFHpA, PFHxA, PFPeA, PFBA, PFPrA, TFA) in *Air test* (A, B), in O_2 *test* (C, D), N_2 *test* (E, F) and N_{2sat} *test* (G, H).

PFOA degradation is expected to produce fluoride ions due to several routes such as dehydrofluorination of primary perfluorinated alcohols and hydrolysis of both COF_2 and perfluoroacyl fluoride intermediates. Overall, fluoride release can be considered as a complementary marker of PFOA mineralization; however, differences in the balance between fluoride yields and mineralization degrees can be noticed and should be ascribed to several contributory causes, such as the volatility of some PFOA decomposition products, like HF and COF_2, the partial fluorination of the TiO_2 catalyst and the undesired production of $SiF_6^{=}$. Fluoride concentration in solution increased linearly during the *Air test* until around 9 h of photoabatement; then F^- increase was less pronounced (Fig. S.I.2-B). At the end of the treatment, the detected fluoride concentration was 29 mM, corresponding to a F^- yield of 48%. Fluoride release in *O_2 test* was definitely quicker than in the case of *Air test* (Fig. S.I.3-B): the F^- concentration reached 25 mM after 4 h which was about 2.5 times the F^- content observed in the *Air test* after the same degradation time (10 mM after 4 h); after 7 h treatment, the F^- concentration reached a *plateau* and a maximum value of 31 mM, slightly higher than the one in the *Air test*. This trend can be ascribed to an almost complete deactivation of the catalyst due to the chemical interactions of fluoride ions with TiO_2 surface moieties [27,28]. In *N_2 test* as well as in *N_{2sat} test*, a limited fluoride release was observed (Fig. S.I.4-B and S.I.5-B): at the end of the tests (after 15 h), [F^-] were about 6 and 3 mM, respectively; F^- yields were around 10% and 5%, respectively. These results confirm that the photocatalytic degradation of fluorinated surfactants in solution is significantly influenced by the presence of dissolved oxygen.

3.3. ^{19}F-NMR results

Referring to the labeled formula $CF_{3(\eta)}CF_{2(\zeta)}CF_{2(\varepsilon)}CF_{2(\delta)}CF_{2(\gamma)}CF_{2(\beta)}CF_{2(\alpha)}COOH$, the assignments of PFOA in the ^{19}F-NMR spectra (Fig. S.I.6) were in agreement with literature: δ = -81.9 (3 F, F_η), -127.1 (2 F, F_ζ), -123.8 (2 F, F_ε), -123.1 (2 F, F_δ), -122.9 (2 F, F_γ), -124.2 (2 F, F_β), -118.5 (2 F, F_α) ppm [52,53]. The peaks of shorter perfluorinated acids ($C_{7\text{-}3}$) have chemical shifts located in the

immediate vicinity of PFOA signals, except for trifluoroacetic acid (TFA) that is characterized by a single signal at -76.55 ppm (generally used as a calibration standard) [28,54,55]. ^{19}F-NMR spectra of PFOA solutions collected from the photoabatement reactor at different times during the kinetic tests (*Air*, *O_2*, *N_{2sat}* and *N_2 tests*) were recorded in order to confirm the variation in the chemical composition of the samples. The integrals of the signals ascribable to $CF_{2(\alpha-\zeta)}$ and $CF_{3(\eta)}$were calculated for each spectra and the corresponding ratios (ϑ) between the sum of $CF_{2(\alpha-\zeta)}$ ^{19}F-NMR integrals and the sum of $CF_{3(\eta)}$ integrals were also evaluated (Table 1): $\vartheta = \sum(CF_{2(\alpha-\zeta)}$ integrals)/$\sum(CF_{3(\eta)}$ integrals). The direct mineralization of PFOA (Eq. 2) progressively reduces the concentrate of the starting acid, formally avoiding the formation of shorter chain species and maintaining constant the ratio ϑ:

$$CF_3(CF_2)_6COOH + 7/2\ O_2 + 7\ H_2O \rightarrow 8\ CO_2 + 15\ HF \qquad (2)$$

On the contrary, if the PFOA decomposition proceeds across intermediates, shorter chain acids are generated and the ^{19}F-NMR integrals ascribable to CF_2 moieties in the chains decrease independently from the terminal CF_3 integrals; thus, the ratio ϑ is expected to decrease.

Table 1. Comparison of ϑ values at different decomposition time for *Air*, *O_2*, *N_2* and *N_{2sat}* kinetic tests.

Test	Time (h)	ϑ (-)	Mineralization (%)[a]
Air test	0	4.0	0
	7	3.7	50
	9	2.9	62
	15	1.6	80
O_2 test	0	4.0	0
	4	3.3	69
	7	2.3	78
N_2 test	0	4.0	0
	7	3.9	30
	15	3.3	54
N_{2sat} test	0	4.0	0
	7	4.0	1
	15	4.0	2

a. % mineralization calculated on the basis of TOC data.

As reported in Table 1, the calculated ϑ value in the starting solution was equal to 4.0. The comparison of ϑ values at similar mineralization degrees in different tests reveals the relative incidence of the two alternative degradation pathways: in particular, low ϑ values can be ascribed to a higher influence of the photo-redox $C_n \rightarrow C_{n-1}$ stepwise mechanism; conversely, experiments characterized by high ϑ values preferably follow the β-scission pathway. In *Air* and *O_2 tests*, the comparison of ϑ values highlighted a well-defined trend; in fact at similar mineralization degrees, ϑ_{Air} were always significantly lower than ϑ_{O2} (Table 1): at mineralization of 62%, ϑ_{Air} at 9 h was equal to 2.9, while ϑ_{O2} at 4 h was 3.3; more markedly, at mineralization of 80% ϑ_{Air} at 15 h was equal to 1.6, that is definitely lower than 2.3 (ϑ_{O2} at 7 h). A similar trend was observed in *Air* and *N_2* tests: at mineralization of 52%, ϑ_{Air} at 7 h was found equal to 3.7 while ϑ_{N2} at 15 h was 3.3.

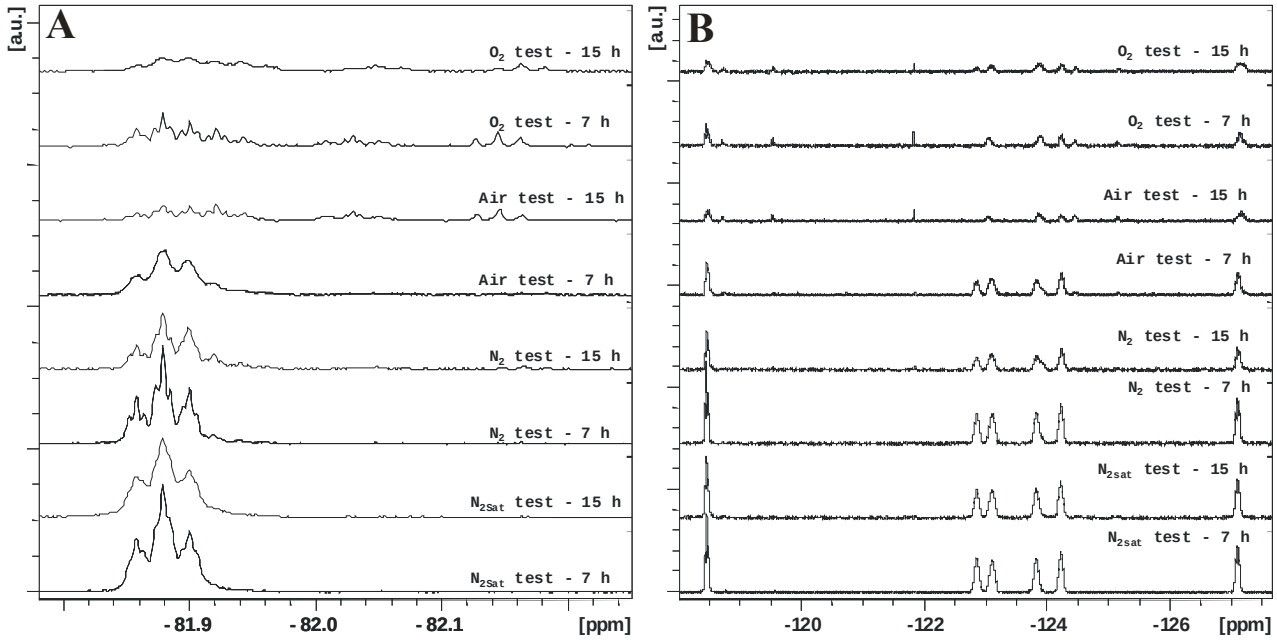

Figure 3. Comparison of ^{19}F-NMR spectra recorded at 7 and 15 h for *Air*, *O_2*, *N_{2sat}* and *N_2* kinetic tests: zooms in the $CF_{3(\eta)}$ (A) and $CF_{2(\alpha\text{-}\zeta)}$ (B) regions.

On the basis of these results it is possible to hypothesize that in the presence of a constant O_2 feed (*O_2 test*) the degradation of PFOA preferentially follows the β-scission pathway. On the contrary, in O_2 starvation conditions (*N_2 test*), the photo-redox $C_n \rightarrow C_{n-1}$ chain length mechanism appears to be

preponderant. In the case of PFOA degradation in the presence of naturally dissolved oxygen (*Air test*), a balanced coexistence of β-scission and photo-redox pathways is possible.

It is also interesting to compare the $CF_{3(\eta)}$ signals obtained at different PFOA mineralization (Fig. 3-A). In the spectra of *Air test* at 15 h and *O_2 test* at both 7 and 15 h, the well-resolved triplet of triplets of the PFOA $CF_{3(\eta)}$ signal at -81.86 ppm varied in multiple signals resulting from the partial overlapping of several contributions: a triplet at -82.15 ppm due to PFPrA, a triplet of triplets at -82.03 ppm due to PFPeA and a multiplet in the range between -81.86 and -81.92 ppm due to overlapping triplets of triplets ascribable to PFOA, PFHpA, PFHxA and PFBA [55-61]. This transition confirmed the coexistence of comparable amounts of different perfluorocarboxylic acids (C_{8-3}). In addition, the presence of TFA (C_2) was also proved by its distinctive signal at -76.55 ppm (Fig. S.I.7-11). Conversely, in the spectra of *N_2* and *N_{2sat} tests* at both 7 and 15 h, the $CF_{3(\eta)}$ signal of PFOA remained almost unchanged (Fig. S.I.12 and S.I.13); in *N_2 test* at 15 h a slight shoulder at -81.92 ppm can be detected. Comparatively, in these tests it was possible to notice a complementary trend in the $CF_{2(\alpha\text{-}\zeta)}$ signals (from -118 to -128 ppm) obtained at different PFOA mineralization (Fig 3-B): in the spectra of *Air test* at 15 h and *O_2 test* at both 7 and 15 h, CF_2 signals almost disappeared and new weak CF_2 signals appeared at -118.7 (triplet; $CF_{2(\alpha)}$ of PFBA), -119.5 (quartet; $CF_{2(\alpha)}$ of PFPrA), -124.5 (multiplet; $CF_{2(\beta)}$ of PFPeA) and -125.2 ppm (multiplet; $CF_{2(\beta)}$ of PFBA), ascribable to low concentration of shorter perfluorocarboxylic acids [55-61]. In *N_2 test* at 15 h and in *Air test* at 7 h, only a broadening of the intense signal of the $CF_{2(\alpha\text{-}\zeta)}$ peaks was observed.

3.3. β-scission of perfluorooxyradicals and carbonyl difluoride detection

The PFOA degradation passes through the formation of oxygen-centered perfluororadicals, as already reported in the literature [28]. The commonly accepted mechanisms foresee that these radicalic intermediates evolve by producing unstable perfluorinated alcohols, which further decompose to perfluoroacyl fluorides by eliminating hydrofluoric acid [65]. However, the β-scission reaction of perfluorinated oxyradicals (C_nO) is thermodynamically favored with a low

kinetic barrier; shorter carbon-centered perfluoroalkyl radicals (C_{n-1}) and COF_2 are formed as reaction products [18]. Perfluoroalkyl radicals continue the degradation pathway and COF_2 is rapidly hydrolyzed in aqueous media by generating CO_2 and HF. To demonstrate this pathway, the hydrolysis of COF_2 should be inhibited by setting the experiment in the absence of water and allowing the release of COF_2 from the reaction environment in gaseous phase. Therefore, a specific test was defined in order to achieve the PFOA degradation in absence of water and to avoid the COF_2 hydrolysis. A high boiling point perfluoropolyether (Galden® HT-170, b.p. = 170°C) was chosen as a solvent because of its solvating properties on PFOA (~ 1,9 g/L), inertness to radicals, stability towards UV-light and low volatility. The remaining experimental parameters of the test were maintained consistent with the *O_2 test* by setting PFOA initial concentration at 4 mM, TiO_2 content at 0.66 g/L, UV-lamp power at 75 W/m^2 and oxygen flux at 7 NL/h. Oxygen was continuously fluxed in the reactor in order to enhance the concentration of perfluorinated peroxyradicals and consequently to facilitate the formation of COF_2. As soon as the PFOA photocatalytic oxidation in the perfluoropolyether solvent started, the outlet gases from the reactor were analyzed by FT-IR spectroscopy and the production of COF_2 was monitored (Fig. 4 and Table S.I.12). The typical IR pattern of COF_2 with the intense signal at 1928 cm^{-1} due to the C=O stretching was easily recognized in the spectra (Fig. S.I.14) [42]. The IR signals of CO_2 antisymmetrical stretching at 2350 cm^{-1} and HF lines in the range 3700-4200 cm^{-1} were also present. A portion of the outlet gases was also analyzed by ^{19}F-NMR spectroscopy and the spectrum revealed an evident signal at -21.5 ppm ascribable to COF_2 (Fig. S.I.15) [52]. While the concentration trends of PFOA degradation intermediates indirectly suggest the existence of two competitive degradation pathways, the detection of COF_2 can be considered as a direct experimental evidence of the β-scissions route in the PFOA degradation mechanism.

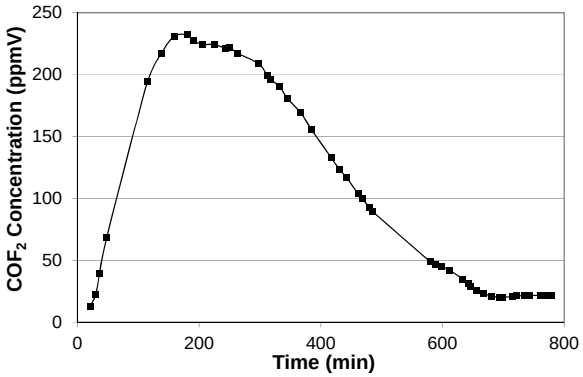

Figure 4. COF_2 concentration (expressed as parts per million by volume, ppmV) in outlet gases during the decomposition of PFOA dissolved in a high boiling point PFPE-based solvent (Galden® HT-170).

In the PFPE-solvent PFOA was completely degraded after approximately 12 h and the maximum COF_2 concentration in the flux resulted equal to 232 ppmV. The COF_2 concentration trend over time revealed the rapid and almost complete decomposition of the PFOA through the β-scission pathway (Fig. 4). In addition, the production of COF_2 and its removal from the reaction environment, due to stripping action by the oxygen flow, reduced the release of fluoride ions in the solution. Thus, TiO_2 deactivation due to fluoride ions was inhibited by performing PFOA photooxidation in a PFPE-based solvent and, even after 15 h of photoabatement only a minor part of the catalyst turned out to be fluorinated. At the end of the test, XPS analysis of TiO_2 catalyst (Fig. S.I.16) showed in the Ti *2p* region two couples of peaks which can be attributed to pure titanium dioxide (at 458-464 eV) and to titanium fluorides with low fluorination degree (at 460-466 eV). On the basis of the deconvolutions, the amount of these fluorinated species was estimated as 30% of the surface composition.

3.4. Suggested mechanism for PFOA photocatalytic oxidation

The experimental results discussed in this work allowed new insights on the PFOA degradation mechanism. In particular, the role of oxygen, the concentration trends of the degradation

intermediates and the detection of COF_2 offer a new interpretation of the photocatalytic oxidation of PFOA.

It is commonly recognized that the PFOA degradation mechanism is initiated with the excitation of titanium dioxide caused by the irradiation of UV light [29,36,66]; after being excited by UV radiation (Fig. 5 - Reaction a), TiO_2 accepts one electron from dissociated PFOA in water ($CF_3(CF_2)_6COO^-$), generating PFOA radical (Fig. 5 - Reaction b) [29,36,66]. As clarified by various papers, PFOA decomposition starts in correspondence to the carboxylic function that undergoes a Kolbe decarboxylation (Fig. 5 - Reaction c) [29,67-69].

$$TiO_2 \xrightarrow{h\upsilon} TiO_2^* (h^+ + e^-) \quad (a)$$

$$CF_3(CF_2)_6COO^- \xrightarrow{h^+} CF_3(CF_2)_6COO\cdot \quad (b)$$

$$CF_3(CF_2)_6COO\cdot \rightarrow CF_3(CF_2)_5CF_2\cdot + CO_2 \quad (c)$$

The energetically favoured reaction of C_7 radicals includes the formation of primary perfluorinated alcohols by coupling with hydroxyl radicals produced by water oxidation due to photo-generated holes ($Ti^{IV}OH\cdot^+$) (Fig. 5 - Reaction d) [70]:

$$CF_3(CF_2)_5CF_2\cdot + OH\cdot \rightarrow CF_3(CF_2)_5CF_2OH \quad (d)$$

However, as demonstrated by the kinetic tests, a high concentration of oxygen in the reaction environment promotes the coupling between C_7 radicals and O_2 by inducing the formation of peroxyradicals (Fig. 5 - Reaction e) [71]:

$$CF_3(CF_2)_5CF_2\cdot + O_2 \rightarrow CF_3(CF_2)_5CF_2OO\cdot \quad (e)$$

The coupling of two peroxyradicals allows the production of oxyradicals (Fig. 5 - Reaction f) that, in the presence of the surface excited electrons of TiO_2 and water, generate an unstable primary perfluorinated alcohol (Fig. 5 - Reaction g) [71,72].

$$2\ CF_3(CF_2)_5CF_2OO\cdot \rightarrow 2\ CF_3(CF_2)_5CF_2O\cdot + O_2 \quad (f)$$

$$CF_3(CF_2)_5CF_2O\cdot + H_2O \xrightarrow{e^-} CF_3(CF_2)_5CF_2OH + OH^- \quad (g)$$

Alternatively, peroxyradicals can react with molecular oxygen originating oxyradicals and releasing ozone that can react with C_7 radicals, generating further oxyradicals [18].

Primary perfluorinated alcohols produced in reactions (d) and (g) are widely reported as thermodynamically unstable (from -80 to -160 kJ/mol) and originate the corresponding acyl fluorides and hydrogen fluoride (Fig. 5 - Reaction h) [68,72]; in the presence of water, the acyl fluorides hydrolyze to carboxylic acids (Fig. 5 - Reaction i) [72-75].

$$CF_3(CF_2)_5CF_2OH \rightarrow CF_3(CF_2)_5C(O)F + HF \quad (h)$$

$$CF_3(CF_2)_5C(O)F + H_2O \rightarrow CF_3(CF_2)_5COOH + HF \quad (i)$$

The reactions from (a) to (i) are at the basis of the stepwise $C_n \rightarrow C_{n-1}$ chain length shortening during PFOA degradation. The evidences obtained from the concentration trends of the degradation intermediates and the detection of COF_2 prove the existence of another reaction pathway, where the oxyradical formed in reaction (f) evolves by eliminating COF_2 through monomolecular β-scission and consequent generation of a C_{n-1} radical [4,76,77]:

$$CF_3(CF_2)_5CF_2O\cdot \rightarrow CF_3(CF_2)_4CF_2\cdot + COF_2 \quad (j)$$

The carbon-centered perfluorinated radical is redirected at the step of reaction (e), while fluorophosgene is quenched in the aqueous environment generating hydrogen fluoride and carbon dioxide [72]. It is remarkable that the mechanism based on β-scissions can promote an almost complete PFOA decomposition without the formation of perfluorinated acids as intermediates. Thus, the key steps of the complete oxidation mechanism are represented by the two competing reactions: the bimolecular reduction of the oxyradical activated by TiO_2 surface (Fig. 5 - Reaction g) and the monomolecular β-scission generating COF_2 and C_{n-1} radical (Fig. 5 - Reaction j).

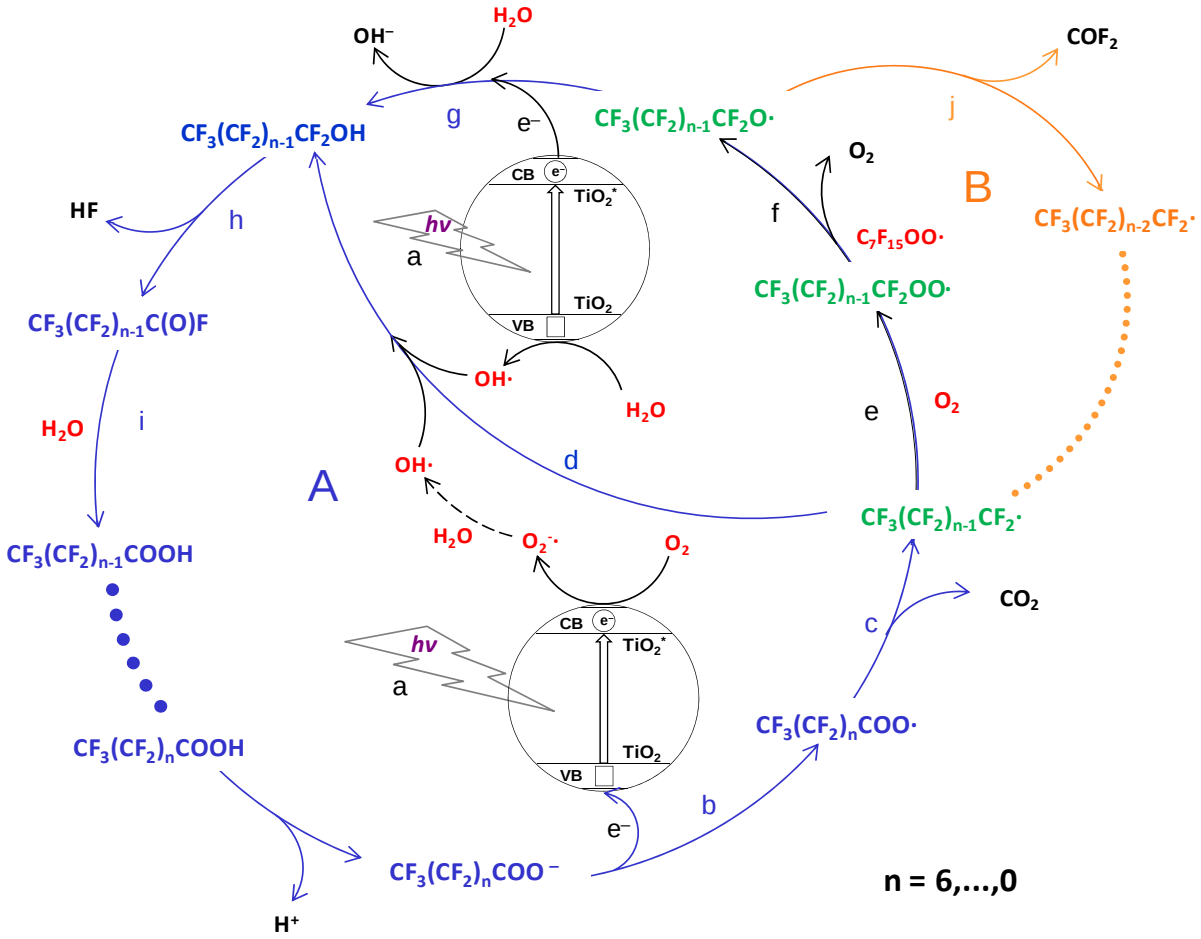

Figure 5. Reaction mechanism of PFOA degradation in the presence of TiO_2 photocatalyst: photo-redox pathway (A - blue arrows); β-scission pathway (B - orange arrows).

4. Conclusions

The photocatalytic oxidation of PFOA promoted by titanium dioxide was studied by testing the reaction in different conditions: static air, oxygen flux, nitrogen flux and pre-saturated nitrogen flux. The effects of oxygen excess or defect in the reaction environment were evaluated in different kinetic tests by measuring mineralization degrees and fluoride releases by TOC analysis and IC, respectively. Concentration trends of PFOA degradation intermediates were also determined by HPLC-MS and ^{19}F-NMR analyses. In particular, the disclosure of very short chain acids at the beginning of the reaction suggested the presence a PFOA oxidation mechanism alternative to the stepwise photo-redox $C_n \rightarrow C_{n-1}$ pathway: the β-scissions routes mediated by COF_2 elimination. The mechanism based on β-scission reactions appeared to be dominant in O_2-enriched solutions,

while in O_2-starving conditions the photo-redox $C_n \rightarrow C_{n-1}$ chain length decrease mechanism prevailed. These hypotheses were confirmed by detecting carbonyl difluoride, COF_2, specifically produced in the β-scission pathway. An appropriate kinetic test was set for COF_2 detection by avoiding its easy hydrolysis and a high boiling point perfluoropolyether as reaction solvent was employed because of the solvating properties on PFOA. Thus, COF_2 production was characterized by ^{19}F-NMR and IR analyses. The production of COF_2 in a non-aqueous medium also reduced the release of fluoride ions in the reaction environment and hindered the F^--induced catalyst deactivation. In addition to the confirmation of the mechanism, it is worth to notice that carbonyl difluoride is an important industrial intermediate and its synthesis with good selectivity and high purity was possible starting from PFOA as pioneering recycling of this banned fluorinated surfactant.

Appendix A. Glossary of acronyms, names (classical and IUPAC) and condensed chemical formulas for PFCAs

PFOA	Perflurooctanoic acid (or perfluorocaprylic acid)	$CF_3(CF_2)_6COOH$
	2,2,3,3,4,4,5,5,6,6,7,7,8,8,8-Pentadecafluorooctanoic acid	
PHpA	Perfluroheptanoic acid (or perfluoroenhantic acid)	$CF_3(CF_2)_5COOH$
	2,2,3,3,4,4,5,5,6,6,7,7,7-Tridecafluoroheptanoic acid	
PFHxA	Perflurohexanoic acid (or perfluorocaproic acid)	$CF_3(CF_2)_4COOH$
	2,2,3,3,4,4,5,5,6,6,6-Undecafluorohexanoic acid	
PFPeA	Perfluropentanoic acid (or perfluorovalerianic acid)	$CF_3(CF_2)_3COOH$
	2,2,3,3,4,4,5,5,5-Nonafluoropentanoic acid	
PFBA	Perflurobutanoic acid (or perfluorobutyric acid)	$CF_3(CF_2)_2COOH$
	2,2,3,3,4,4,4-Heptafluorobutanoic acid	
PFPrA	Perfluropropanoic acid (or perfluoropropionic acid)	CF_3CF_2COOH
	2,2,3,3,3-Pentafluoropropanoic acid	

TFA	Trifluoroethanoic acid (or trifluoroacetic acid) *2,2,2-Trifluoroethanoic acid*	CF_3COOH

Acknowledgments

The authors wish to acknowledge with thanks the generous support and the valuable interactions induced to this research in the field of fluorinated materials by the institution of the Politecnico di Milano/Solvay Fluorine Chemistry Chair. This work has been supported by MIUR (PRIN 2010-2011, prot. 2010PFLRJR).

References

[1] J. G. Drobny, Technology of Fluoropolymer, second ed., CRC Press, Boca Raton, 2009.

[2] W. Navarrini, M. V. Diamanti, M. Sansotera, F. Persico, M. Wu, L. Magagnin, S. Radice, Prog. Org. Coat. 74 (2012) 794-800.

[3] F. Persico, M. Sansotera, C. L. Bianchi, C. Cavallotti, W. Navarrini, Appl. Catal., B 170 (2015) 83-89.

[4] M. Avataneo, W. Navarrini, U. De Patto, G. Marchionni, J. Fluorine Chem. 130 (2009) 933-937.

[5] C. Cornelis, W. D'Hollander, L. Roosens, A. Covaci, R. Smolders, R. Van den Heuvel, E. Govarts, K. Van Campenhout, H. Reynders, L. Bervoets, Chemosphere 86 (2012) 308-314.

[6] J. H. Johansson, U. Berger, R. Vestergren, I. T. Cousins, A. Bignert, A. Glynn, P. O. Darnerud, Environ. Pollut. 188 (2014) 102-108.

[7] R. C. Buck, J. Franklin, U. Berger, J. M. Conder, I. T. Cousins, P. de Voogt, A. A. Jensen, K. Kannan, S. A. Mabury, S. P. J. van Leeuwen, Integr. Environ. Assess. Manag. 7 (2011) 513-541.

[8] E. Smulders, W. Von Rybinski, A. Nordskog, Laundry Detergents. Ullmann's Encyclopedia of Industrial Chemistry, seventh ed., Wiley-VCH, Weinheim, 2011.

[9] C. A. Moody, J. A. Field, Environ. Sci. Technol. 34 (2000) 3864-3870.

[10] A. Singh, J. D. Van Hamme, O. P. Ward, Biotechnol. Adv. 25 (2007) 99-121.

[11] G. Kostov, F. Boschet, B. Ameduri, J. Fluorine Chem. 130 (2009) 1192-1199.

[12] G. Boutevin, D. Tiffes, C. Loubat, B. Boutevin, B. Ameduri, J. Fluorine Chem. 134 (2012) 77-84.

[13] G. Marchionni, V. Tortelli, I. Wlassics, V. Kapeliouchko, US 8703889 B2 (2014).

[14] M. A. Guerra, K. Hintzer, M. Jurgens, H. Kaspar, A. R. Maurer, G. I. Moore, Z. M. Qiu, J. F. Schulz, W. Schwertfeger, T. Zipplies, US 0276103 A1 (2007).

[15] T. Ishikawa, N. Tsuda, Y. Yamamoto, US 7777075 B2 (2010).

[16] J. Hoshikawa, S. Higuchi, Y. Matsuoka, N. Yamagishi US 7709566 B2 (2010).

[17] P. D. Brothers, S. V. Gangal US 7932333 B2 (2011).

[18] J. Niu, H. Lin, C. Gong, X. Sun, Environ. Sci. Technol. 47 (2013) 14341-14349.

[19] S. M. Mitchell, M. Ahmad, A. L. Teel, R. J. Watts, Environ. Sci. Technol. Lett. 1 (2014) 117-121.

[20] J. C. Lin, S. L. Lo, C. Y. Hub, Y. C. Lee, J. Kuo, Ultrason. Sonochem. 22 (2015) 542-547.

[21] N. Takeuchi, Y. Kitagawa, A. Kosugi, K. Tachibana, H. Obo, K. Yasuoka, J. Phys. D: Appl. Phys. 47 (2014) 045203.

[22] Y. Lee, S. Lo, J. Kuo, C. Hsieh, Front. Environ. Sci. Eng. 6 (2012) 17-25.

[23] W. Yuan, P. Zhang, J. Environ. Sci. 26 (2014) 2207-2214.

[24] R. R. Giri, H. Ozaki, T. Okada, S. Taniguchi, R. Takanami, Chem. Eng. J. 180 (2012) 197-203.

[25] M. J. Chen, S. L. Lo, Y. C. Lee, C. C. Huang, J. Hazard. Mater. 288 (2015) 168-175.

[26] B. Zhao, X. Li, L. Yang, F. Wang, J. Li, W. Xia, W. Li, L. Zhou, C. Zhao, Photochem. Photobiol. 91 (2015) 42-47.

[27] M. Sansotera, F. Persico, C. Pirola, W. Navarrini, A. Di Michele, C. L. Bianchi, Appl. Catal., B 148 (2014) 29-35.

[28] S. Gatto, M. Sansotera, F. Persico, M. Gola, C. Pirola, W. Panzeri, W. Navarrini, C. L. Bianchi, Catal. Today 241 (2015) 8-14.

[29] S. C. Panchangam, A. Y. C. Lin, J. H. Tsai, C. F. Lin, Chemosphere 75 (2009) 654-660.

[30] C. D. Vecitis, H. Park, J. Cheng, B. T. Mader, M. R. Hoffmann, Front. Environ. Sci. Eng. China 3 (2009) 129-151.

[31] J. Liu, S. M. Avendaño, Environ. Int. 61 (2013) 98-114.

[32] Z. Wang, I. T. Cousins, M. Scheringer, K. Hungerbühler, Environ. Int. 60 (2013) 242-248.

[33] D. Friedmann, C. Mendive, D. Bahnemann, Appl. Catal., B 99 (2010) 398-406.

[34] O. Carp, C. L. Huisman, A. Reller, Prog. Solid State Chem. 32 (2004) 33-177.

[35] N. Serpone, J. Photochem. Photobiol. A 104 (1997) 1-12.

[36] A. Fujishima, T. N. Rao, D. A. Tryk, J. Photochem. Photobiol. C 1 (2000) 1-21.

[37] K. Sato, T. Hirakawa, A. Komano, S. Kishi, C. K. Nishimoto, N. Mera, M. Kugishima, T. Sanoa, H. Ichinose, N. Negishi, Y. Seto, K. Takeuchi, Appl. Catal., B 106 (2011) 316-322.

[38] S. R. Seagle in: J. I. Kroschwitz (Ed.), The Kirk-Othmer Encyclopedia of Chemical Technology, Vol. 24, fourth ed., John Wiley and Sons, New York, 1997, pp. 186-224.

[39] N. P. Mellott, C. Durucan, C. G. Pantano, M. Guglielmi, Thin Solid Films 502 (2006) 112-120.

[40] P. Pichat, in: E. Pelizzetti, N. Serpone (Eds.), Homogeneous and Heterogeneous Photocatalysis, Vol. 174, NATO ASI Series, Springer, New York/Heidelberg, 1986, pp. 533-554.

[41] J. Pacansky, R. J. Waltman, J. Phys. Chem. 95 (1991) 1512-1518.

[42] V. Francesco, M. Sansotera, W. Navarrini, J. Fluorine Chem. 155 (2013) 2-20.

[43] W. Navarrini, V. Tortelli, A. Russo, S. Corti, J. Fluorine Chem. 95 (1999) 27-39.

[44] W. Navarrini, A. Russo, V. Tortelli , J. Org. Chem. 60 (1995) 6441-6443.

[45] M. Sansotera, W. Navarrini, M. Gola, C. L. Bianchi, P. Wormald, A. Famulari, M. Avataneo, J. Fluorine Chem. 132 (2011) 1254-1261.

[46] W. Navarrini, C. L. Bianchi, L. Magagnin, L. Nobili, G. Carignano, P. Metrangolo, G. Resnati, M. Sansotera, Diam. Relat. Mater. 19 (2010) 336-341.

[47] U. Järnberg, K. Holmström, B. van Bavel, A. Kärrman, Perfluoroalkylated acids and related compounds (PFAS) in the Swedish environment - Chemistry, Sources & Exposure. Report to Swedish Environment Protection Agency (2006).

[48] C. Gambarotti, C. Punta, F. Recupero, T. Caronna, L. Palmisano, Curr. Org. Chem. 14 (2010) 1153-1169.

[49] S. Brosillon, L. Lhomme, C. Vallet, A. Bouzaza, D. Wolbert, Appl. Catal., B 78 (2008) 232-241.

[50] J. B. Heredia, J. Torregrosa, J. R. Dominguez, J. A. Peres, J. Hazard. Mater. 83 (2001) 255-264.

[51] P. Švec, A. Eisner, L. Kolářová, T. Weidlich, V. Pejchal, A. Růžička, Tetrahedron Lett. 49 (2008) 6320-6323.

[52] B. Ameduri, Chem. Rev. 109 (2009) 6632-6686.

[53] A. H. Karoyo, A. S. Borisov, L. D. Wilson, P. Hazendonk, J. Phys. Chem. B 115 (2011) 9511-9527.

[54] A. A. Ribeiro, J. Fluorine Chem. 83 (1997) 61-66.

[55] W. R. Dolbier, Guide to Fluorine NMR for Organic Chemists, Wiley, Hoboken, 2009.

[56] G. Filipovich, G. V. D. Tiers, J. Phys. Chem. 63 (1959) 761-763.

[57] D. O. Graham, W. B. McCormack, J. Org. Chem. 31 (1966) 958-959.

[58] C. Dapremont-Avignon, P. Calas, A. Commeyras, C. Amatore, J. Fluorine Chem. 51 (1991) 357-379.

[59] D. A. Ellis, K. A. Denkenberger, T. E. Burrow, S. A. Mabury, J. Phys. Chem. A 108 (2004) 10099-10106.

[60] A. A. Ribeiro, K. Umayahara, Magn. Reson. Chem. 41 (2003) 107-114.

[61] N. Ilayaraja, A. Manivel, D. Velayutham, M. Noel, J. Appl. Electrochem. 38 (2008) 175-186.

[62] Z. Liu, J. D. Goddard, J. Phys. Chem. A 113 (2009) 13921-13931.

[63] R. D. Chambers in: R. D. Chambers (Ed.), Fluorine in Organic Chemistry, Blackwell Publishing Ltd., Oxford, 2004, pp. 236-295.

[64] A. Mills, S. Le Hunte, J. Photochem. Photobiol. A 108 (1997) 1-35.

[65] H. Hori, E. Hayakawa, H. Einaga, S. Kutsuna, K. Koike, T. Ibusuki, H. Kiatagawa, R. Arakawa, Environ. Sci. Technol. 38 (2004) 6118-6124.

[66] Y. Wang, P. Zhang, J. Hazard. Mater. 192 (2011) 1869-1875.

[67] H. Hori, A. Yamamoto, E. Hayakawa, S. Taniyasu, N. Yamashita, S. Kutsuna, Environ. Sci. Technol. 39 (2005) 2383-2388.

[68] C. Gong, X. Sun, C. Zhang, X. Zhang, J. Niu, Int. J. Mol. Sci. 15 (2014) 14153-14165.

[69] H. Lin, J. Niu, S. Ding, L. Zhang, Wat. Res. 46 (2012) 2281-2289.

[70] S. Kutsuna, H. Hori, Int. J. Chem. Kinet. 39 (2007) 276-288.

[71] C. Kormann, D. W. Bahnemann, M. R. Hoffmann, Environ. Sci. Technol. 25 (1991) 494-500.

[72] M. Sansotera, W. Navarrini, G. Resnati, P. Metrangolo, A. Famulari, C. L. Bianchi, P. A. Guarda, Carbon 48 (2010) 4382-4390.

[73] W. J. De Bruyn, J. A. Shorter, P. Davidovits, D. R. Worsnop, M. S. Zahniser, C. E. Kolb, Environ. Sci. Technol. 29 (1995) 1179-1185.

[74] A. M. B. Giessing, A. Feilberg, T. E. Mögelberg, J. Sehested, M. Bilde, T. J. Wallington, O. J. Nielsen, J. Phys. Chem. 100 (1996) 6572-6579.

[75] M. Sansotera, W. Navarrini, L. Magagnin, C. L. Bianchi, A. Sanguineti, P. Metrangolo, G. Resnati, J. Mater. Chem. 20 (2010) 8607-8616.